EMBJ.ORG FOR YOUNG DOCTORS

EUROMEDITERRANEAN BIOMEDICAL JOURNAL
2017,12 (07) 029–035
(*FORMERLY: CAPSULA EBURNEA*)

Original article

NOVEL INTRONIC VARIANTS IN UNCONVENTIONAL GENE CLUSTER COULD LEAD TO THE IDENTIFICATION OF A NEW RETINITIS PIGMENTOSA PHENOTYPE

Luigi Donato [1, 2]

1. *Department of Biomedical and Dental Sciences and Morphofunctional Imaging, Division of Medical Biotechnologies and Preventive Medicine, University of Messina, Messina, Italy.*
2. *Department of Cutting-Edge Medicine and Therapies, Biomolecular Strategies and Neuroscience, Section of Neuroscience-applied Molecular Genetics and Predictive Medicine, I. E. ME. S. T., Palermo, Italy.*

ARTICLE INFO

Article history:
Received 05January 2017
Revised 13 February 2017
Accepted 02 March 2017

Keywords:
Retinal dystrophies, polymorphisms,
Next generation sequencies, predictions.

ABSTRACT

The Retinitis pigmentosa (RP) is an inherited heterogeneous ocular disorder characterized by progressive retinal degeneration. Although at least 50 genes are known to be causative of RP, many others are still unidentified. We describe a Sicilian female patient affected by an unknown form of RP. She was screened by Whole Genome Sequencing, and the subsequent variant analysis was integrated with filtering and pathway analysis and enrichment. Finally, the relevant variants were analyzed *in silico* to establish their potential effects. Based on previous analyses, 15 intronic variants, distributed across 6 genes (*EYS, PPEF2, RNF144B, RDH13, FLT3* and *MYO7A*), were selected as potential candidates for disease association. Finally, the consequent *in silico* analysis highlighted their possible role in splicing alterations. The involvement of these genes in the pathogenesis of RP and the newly discovered role of splicing alteration events may offer new insights into the diagnosis of unknown forms of retinitis pigmentosa.

1. Introduction

Retinitis pigmentosa (RP) is an inherited heterogeneous ocular disorder characterized by progressive retinal degeneration [1]. It affects both eyes and involves the retinal pigment epithelium (RPE) and photoreceptors (PRs), leading to a slow and progressive death of these cells [2]. Since PRs, like other retinal cells, are neural cells, their loss impairs the transmission of visual information to the brain [3]. The symptomatology consists of night blindness and a growing deterioration of the visual field, perceived as tunnel vision, principally due to rod PR degeneration. The subsequent involvement of the cone PRs at a later stage could lead to severe alterations of color perception. The clinical hallmarks of this condition include the characteristic mottled appearance of the RPE (usually during the advanced states of the disease), pallor of the optic disc, and shrinking of the retinal blood vessels. [4]. The prevalence of RP varies within different ethnic groups, reaching 1 in 4,000 people in the United States and 1-5 in 10,000 in Italy. The progression rate of the disease and the age of onset of the first symptoms vary depending on many factors, including the genetic transmission patterns [5]. By now, at least 50 genes involved in the activation/inactivation of phototransduction and the related pathways (such as the canonical retinoid cycle in rods - twilight vision - and cones - daylight vision -, ABC transporters coding genes, also involved in other nervous pathologies [6], and cargo trafficking to the periciliary membrane), are known to be causative of different forms of retinitis pigmentosa [7]. Mutations in these genes may be inherited in an autosomal recessive (50-60%), dominant (30-40%) or X-linked (5-20%) pattern, but about 30% is occur in sporadic form [8], frequently with incomplete penetrance and variable clinical expression (like other cerebral diseases [9]). Moreover, many forms of RP that present multisystemic involvement, such as the Bardet-Biedl syndrome that is nowadays treated with steroids [10], are also associated with other rare pathologies like trimethylaminuria [11]. However, the greatest current challenge is the identification of other unknown genes potentially causative of many yet unidentified forms of retinitis pigmentosa [12]. Thanks to the Next Generation Sequencing (NGS) technique, novel disease-causing or -associated genes, as well as strong genotype-phenotype correlations can be identified (about 30-60% of RP cases have

* *Corresponding author*: Luigi Donato, ldonato@unime.it
DOI: 10.3269/1970-5492.2017.12.7
 ISSN: 2279-7165 - Available on-line at www.embj.org

already been characterized [1]), leading to significant improvement of our understanding of allele pathogenicity, protein function and population genetics. In this paper, we present a Sicilian patient affected by an unknown form of RP, screened by Whole Genome Sequencing (WGS). This high-throughput analysis enabled us to amplify the mutational spectrum, identifying not only exonic variants but also intronic ones throughout the entire genome, thereby accurately portraying their impact on splicing.

2. Material and methods

Clinical data

A 70-year-old Sicilian female patient, affected by an unknown form of RP, was recruited at the Policlinico Universitario hospital of Messina. The patient's diagnosis was determined through the following evaluations: fundus analysis, fundus autofluorescence (FAF), infrared reflectance imaging (IR), optical coherent tomography (OCT), visual field (VF), ISCEV electroretinography (ERG) and pattern electroretinogram (PERG). Fundus examination revealed rounded macular and perimacular pigment deposits with sharp edges, confirmed by IR and FAF. ERG revealed a generalized rod impairment with cone involvement (reduced photopic and scotopic responses), with a delay in visual response (PERG with hypovolted P50 wave and increased latency). VF showed central scotoma correlating with outer retinal subfoveal atrophy, observed on FAF and OCT. The study followed the tenets of the Declaration of Helsinki and was approved by the Scientific Ethics Committee of the Azienda Ospedaliera Universitaria - Policlinico "G. Martino" Messina.
Informed consent was signed by patient after a thorough explanation of the nature and possible consequences of the study.

Next Generation Sequencing design

DNA extraction
Genomic DNA was extracted from peripheral blood using QIAamp DNA Mini Kit (Qiagen), and then quantified with a NanoPhotometer P-330 (Implen). DNA integrity was evaluated by visual inspection on a 1% agarose gel.

ION proton sequencing
Workflow for Ion Proton Sequencing can be outlined in three different steps:
1)Fragment library preparation: 1,2 ug of gDNA were fragmented by Ion Xpress™ Plus Fragment Library Kit (ThermoFisher Scientific), using a digestion time of 10 minutes, followed with purification by Agencourt® AMPure® XP Reagent (Beckman Coulter); fragmentation status was tested by Bioanalyzer using the Agilent® High Sensitivity DNA Kit. A nonbarcoded library was obtained using an Ion Plus Fragment Library Kit (ThermoFisher Scientific), according to the manufacturer's procedure. Subsequently, the library was again purified. Size selection was performed with an E-Gel® SizeSelect™ Agarose Gel (ThermoFisher Scientific) using 50-bp DNA Ladder: 150 bp and 200 bp fragments were captured. The two libraries were individually quantified with a Real-time StepOne™ Plus System, with Ion Library Quantitation Kit (ThermoFisher Scientific). No library amplifications were performed.
2)Clonal amplification: an equimolar 11pM quantity of both libraries was amplified by Ion PI™ Template OT2 200 Kit v3 using an Ion OneTouch™ 2 Instrument (ThermoFisher Scientific). Emulsion PCR was carried out with microbeads, called Ion Sphere Particles (ISPs). To evaluate the presence of polyclonal sequence amplification, the ISPs obtained were qualitatively checked by Ion Sphere Quality Control kit on a Qubit® 2.0 instrument. ISP enrichment was performed on an Ion OneTouch™ ES instrument (ThermoFisher Scientific).
3)Sequencing run: three v2 Ion PI Chips were run on an Ion Proton™ System (ThermoFisher Scientific); the sequencing run was performed using the Ion PI Sequencing 200 Kit v2.

Read mapping
Generated sequences were processed using the CLC Genomics Workbench 9.5.1 bioinformatics software (CLC bio, Aarhus, Denmark). In CLC workflow, the generated FASTQ files were imported into the software and processed via the following steps: 1) Sequence quality trimming based on Phred quality scores (minimal score = 27) and removal of ambiguous base-calls; 2) Read Mapping (human reference sequence HG19) with <2 mismatches/100bp for alignment; 3) Read Mapping coverage analysis, designed to identify regions indicative of a deletion or an amplification in the sample.

Variant calling
Variant calling was performed using the Fixed Ploidy Variant Detection tool to detect variants with a probability exceeding 90%, using a specific remove pyro-error variants filter set. This tool detects Single Nucleotide Variants (SNVs), Multiple Nucleotide Variants (MNVs), insertions, and deletions, as well as replacements (combinations of neighboring insertions, deletions and SNVs for which the positions are ambiguous), whose representation in the reads is in accordance with the assumed ploidy; it discards variants whose representation in the reads is likely to be due to sequencing errors or mapping artefacts.
The variant caller was set to exclude variants available in broken read pairs, unspecific read alignments as well as variants exclusively found in forward/reverse reads. Finally, InDels and Structural Variants calling was performed, in order to identify structural variants such as contemporary insertions/deletions, inversions, translocations and tandem duplications in read mappings.

Filtering known variants
At the outset, a comparison with known variants from various genomic databases (dbSNP, 1000 genomes, HapMap) was carried out to determine if the variants found had already been investigated.

Pathway analysis and functional enrichment
We selected candidate variants based on their presence in genes with a known correlation with the biological processes involving the eye and/or ocular diseases. This filtering was carried out by Cytoscape (v3.4) and its

GeneMANIA plugin (v3.4.1). Finally, a pathway enrichment analysis was performed by Cytoscape (v3.4) and its ClueGO plugin (v2.2.6), based on GO, KEGG and Reactome [13].
Subcellular locations, biological processes' molecular function and KEGG pathways, from which electronic annotation and experimental were inferred data, were all within the identified GO categories.

Sanger validation of selected variants
Amplification of gene fragments with selected variants was performed using primer pairs designed according to the published nucleotide sequence of GenBank (available upon request). PCR mix was prepared adding 8 µg of genomic DNA to 50µl reaction mixture, containing a 0.2 µm concentration of each primer and 1 U MyTaq polymerase (Bioline). PCR was carried out in a thermal cycler (Gene Amp PCR System 2700; PE Applied Biosystems, Foster City, CA) under the following conditions: denaturation at 95°C for 15 secs, annealing at 49.5°C for 15 secs and extension at 72°C for 10 secs for 35 cycles, after an initial 1 min denaturation at 95 °C.
PCR products were sequenced by direct sequencing with a BigDye Terminator v1.1 Cycle Sequencing kit on a 310 ABI PRISM Sequencer Analyzer (Applied Biosystems, Foster City, CA).

Splicing variant effects prediction
Finally, we assessed the potential negative effects of the intronic variants that were identified through NGS and passed the various filtering and pathway analyses.
The possible creation of ESS sequences, the abolition of ESE sequences, as well as the abolition and creation of canonical sites and cryptic splice sites respectively, were analyzed through an in silico approach with the help of the Human Splicing Finder web-based software (http://www.umd.be/HSF3/HSF.html).

3. Results

Whole genome sequencing was performed on proband with 3 chips using an Ion Torrent Proton instrument. In total, 97.443.256 single-end reads (mean read length ~ 137 bp) were generated, with ~98 % of them mapped, reaching an average quality score (Phred score) of nearly 32 per read, allowing the identification of SNPs and new mutations. A total of 36.271 variants, including 27.456 SNVs, were identified throughout the whole analyzed genome, after passing quality and homopolymeric filters. No variants previously considered causative of or associated with RP were found. According to pathway analyses conducted by Cytoscape and its GeneMANIA and ClueGO plugins, which highlighted functional effects, eye localization and ocular disease affinity, 15 candidate pathogenic variants, distributed in 6 genes (EYS, PPEF2, RNF144B, RDH13, FLT3 and MYO7A), were selected (Table 1). These genes resulted linked to each other in co-expression, co-localization, and genetic and physical interaction networks (Figure 1), suggesting a possible involvement in common pathways.

GENE	VARIANT NAME	POSITION	VARIANT EFFECT	GMAF	AFR_MAF	AMR_MAF	EAS_MAF	EUR_MAF	SAS_MAF	LoFtool	GENOTYPE
EYS	rs372350441	c.5644+58659_5644+58673delATAAAATAAAATAAA	Intron	/	/	/	/	/	/	0.0537	ET
	rs149849078	c.5644+58830_5644+58832delCAA	Intron	/	/	/	/	/	/	0.0537	ET
	rs71638759	c.3443+18021_3443+18024delACCA	Intron	/	/	/	/	/	/	0.0537	ET
	rs112160251	c.3443+18142delT	Intron	/	/	/	/	/	/	0.0537	ET
PPEF2	rs12498639	c.580-718A>C	Intron	T:0.1378	G:0.5378	G:0.9467	G:0.9891	G:0.9821	G:0.9867	0.831	OM
	rs1566975	c.580-65G>A	Intron	C:0.1378	T:0.5378	T:0.9467	T:0.9891	T:0.9821	T:0.9867	0.831	OM
	rs1976517	c.580-49C>T	Non coding transcript exon variant	G:0.1376	A:0.5386	A:0.9467	A:0.9891	A:0.9821	A:0.9867	0.831	OM
	rs1976518	c.591G>A	Synonymous variant	C:0.1378	T:0.5378	T:0.9467	T:0.9891	T:0.9821	T:0.9867	0.831	OM
	rs34238193	c.746+168_746+169dupAA	Intron	A:0.3201	A:0.5378	A:0.7277	A:0.7560	A:0.7097	A:0.7290	0.831	ET
RNF144B	rs1886248	c.-36-336C>T	Intron	C:0.3638	T:0.4713	T:0.6787	T:0.7768	T:0.6302	T:0.6902	0.644	OM
RDH13	rs2569514	c.*849+397C>T	Non coding transcript exon variant	A:0.4551	A:0.3646	A:0.4164	A:0.5685	A:0.5358	A:0.4049	0.318	OM
	rs2569513	c.*849+470C>T	Non coding transcript exon variant	G:0.1745	A:0.6838	A:0.8905	A:0.9692	A:0.8449	A:0.8027	0.318	OM
FLT3	rs17086226	c.2541+58A>G	Intron	C:0.2490	C:0.1467	C:0.2176	C:0.2510	C:0.2107	C:0.4468	0.218	ET
MYO7A	rs7121485	c.-46-926A>G	Intron	A:0.4856	A:0.4924	A:0.6110	A:0.4405	A:0.5606	A:0.3569	0.026	ET
	rs2276283	c.1936-23G>A	Intron	G:0.1943	G:0.1059	G:0.3804	G:0.0516	G:0.3817	G:0.1360	0.026	ET

Table 1 - List of candidate variants, with main characteristics and patient's related genotypes. LoFtool=rank of genic intolerance; the lower the LoFtool gene score percentile, the more intolerant is the gene to functional variation. GMAF=Non-reference allele and frequency of existing variant in 1000 Genomes. AFR_MAF=Non-reference allele and frequency of existing variant in 1000 Genomes combined African population. AMR_MAF =Non-reference allele and frequency of existing variant in 1000 Genomes combined American population. ASN_MAF=Non-reference allele and frequency of existing variant in 1000 Genomes combined Asian population. EAS_MAF=Non-reference allele and frequency of existing variant in 1000 Genomes combined East Asian population. EUR_MAF=Non-reference allele and frequency of existing variant in 1000 Genomes combined European population. SAS_MAF=Non-reference allele and frequency of existing variant in 1000 Genomes combined South Asian population. ET=Heterozygous genotype. OM=Homozygous genotype.

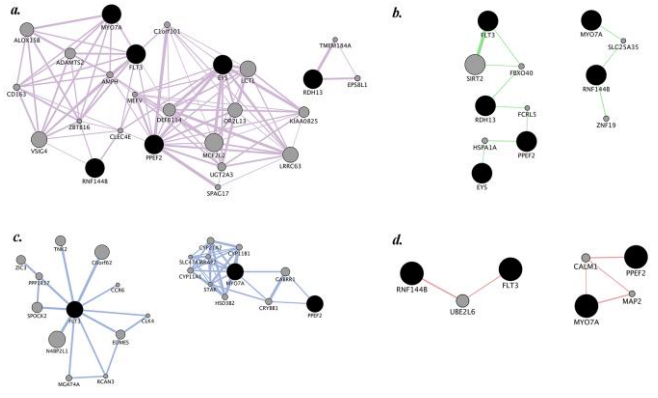

Figure 1 - Pathway analysis with Cytoscape and its GENEmania plugin. Results show how selected candidate variants are linked to each other in co-expression (a), genetic interaction (b), co-localization (c) and physical interaction (d) networks.

The ClueGO analysis permitted us to discover these metabolic and biochemical pathways, primarily involving photoreceptor cell development and detection of light stimulus involved in visual perception, subsequently subcategorized into 37 hierarchically structured GO classifications (Figure 2).

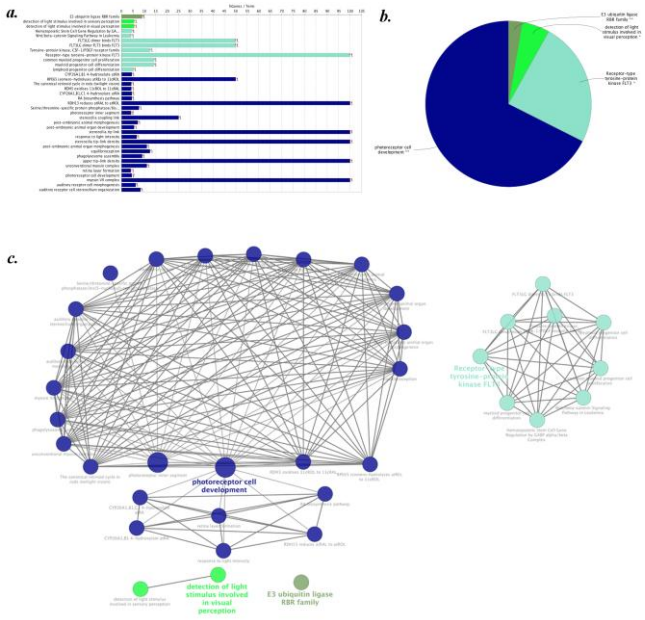

Figure 2 - ClueGO enrichment analysis. Panel shows common metabolic and biochemical pathways involving the examined genes. Pie chart (b) highlighting the prevalence of vision-related pathways, subcategorized into a bar chart (a) representing the percentage of single genes' involvement. Edges and nodes graphic (c) of (a) and (b) merged.

Corroborated by these data, all chosen variants were validated by Sanger sequencing. Finally, since all analyzed variants consisted of intronic polymorphisms, a possible involvement in splicing was hypothesized, due to a potential alteration determined by their presence in corresponding genes. The web-based bioinformatics platform Human Splicing Finder highlighted the alteration of several ESE (exonic splicing enhancer) and ESS (exonic splicing silencer) sites, as well as of branch points (Figure 3), leading us to postulate a possible role of these variants in modifying the splicing process (Figure 4).

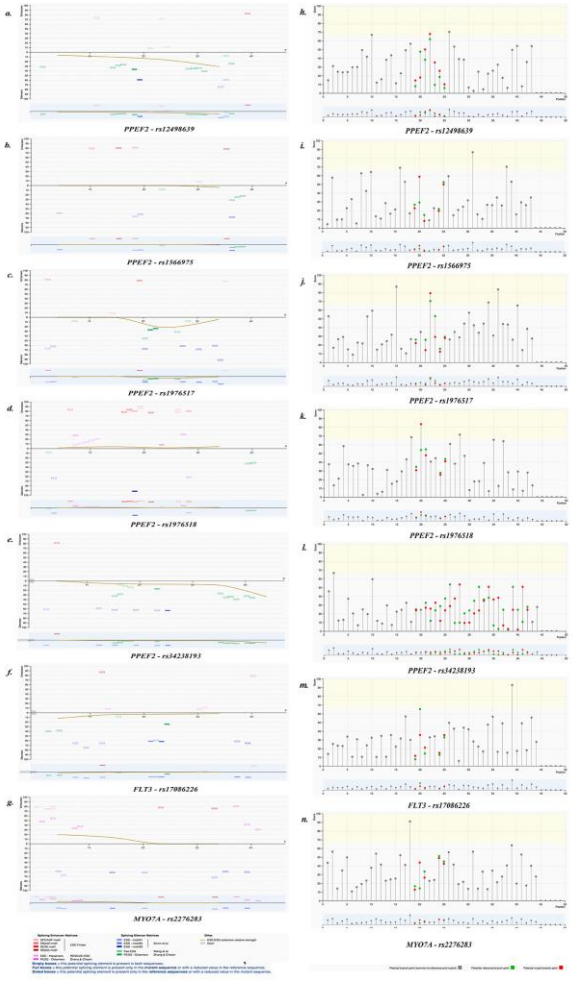

Figure 3 - Alteration of ESE (exonic splicing enhancer) or ESS (exonic splicing silencer) sites (a-g) and branch points (h-n), due to candidate variant presence, derived from all applied algorithms. Empty boxes=this potential splicing element is present in both sequences. Full boxes=this potential splicing element is present only in the mutant sequence or with a reduced value in the reference sequence. Doted boxes=this potential splicing element is present only in the reference sequence or with a reduced value in the mutant sequence.

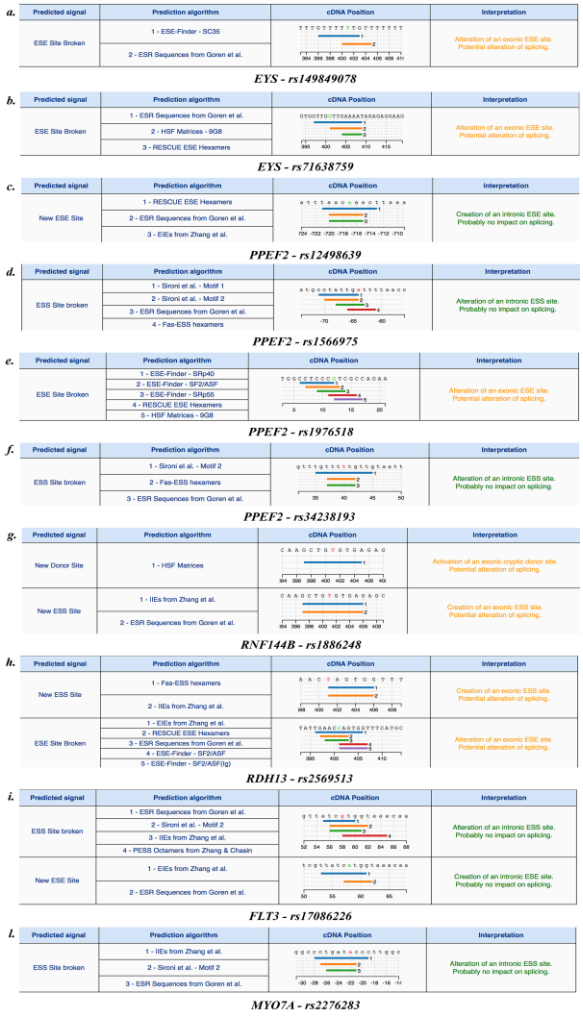

Figure 4 - Possible consequences of altered splicing process caused by the presence of a candidate variant. Predicted signal=indicates the type of signal altered by the mutation. It could be a broken wild type splice site (donor or acceptor), a new cryptic site (donor or acceptor), a broken wild type branch point, an auxiliary splicing signal broken or created (ESE or ESS). Prediction algorithm=this section displays the algorithm(s) that predicted the alteration. The little number preceding the algorithm name indicates the graphic representation of the signal in the next column. cDNA Position=displays a graphic representation of the region in which the mutation occurs. If two or more algorithms predicted the same signal, each of them appear with a line in different color (position and motif length can differ from one algorithm to another). On the top part of the graph, the sequence is represented with the wildtype nt in green (broken site) or the mutant nt in red (new site created). Finally, the values on the x axis of the graphs represent exonic (positive values) or intronic (negative values) variations. Interpretation=explanation about the predicted signal and its possible effect on splicing.

A separate analysis performed on deep intron variants, the results of which are shown in Table 2, offered more detailed information. This approach was employed to further confirm the postulated involvement of these variants in the disease processes.

GENE	VARIANT	POTENTIAL SPLICE SITES					BRANCH POINTS		ENHANCERS MOTIFS (ESS)	SILENCERS MOTIFS	OTHERS
		Splicing Site Type (HFS)	Max Variation (%)	Estimate Exon lenght variation (bp)	Motif Changed (MAXENT)	Max Variation (%)	N° of Potential Altered Branch Points	Average Variation (%)	ESE Variations for SRp40, SC35, SF2/ASF and SRp55 proteins (%) and New/Broken ESE Sites	PESS Octamers, Fas and IIEs from Zhang Algorithms	Exonic Splicing Regulatory Sequences from Goren et al.
EYS	rs372350441	1 Donor (-)	-3.6	-397	3' Motif = 1 Changed	-3128.13	16 New 16 Broken	250/-55	+10	3 New/14 Broken Sites	3 Broken Sites
	rs149849078	2 Acceptors (+)	9.37	-616	3' Motif = 4 Changed	-468.82	19 New 17 Broken	350/-70	+13 and 1 Site Broken	7 New/3 Broken Sites	1 Broken Site
	rs71638759	2 Acceptors (+) 2 Donors (-)	+ 16 and -62	-400	5' Motif = 1 Changed	-488.11	14 New 12 Broken	450/-75	+12 and 3 Broken/3 New Sites	4 Broken Sites	1 New/3 Broken Sites
	rs112160251	/	/	/	/	/	9 New 9 Broken	350/-55	+9 and 1 Broken Site	/	1 New/3 Broken Sites
RNF144B	rs1886248	2 Acceptors (-) 2 Donor (+)	+62 and -1	-397	5' Motif = 2 Changed	-234.71	/	/	+13 and 1 Broken/3 New Sites	4 New Sites	3 New Sites
RDH13	rs2569514	/	/	/			/	/	+8 and 1 Broken Site	1 New Site	/
	rs2569513	1 Acceptor (-)	-9.4	-392	3' Motif = 1 Changed	+0.24	/	/	+7 and 3 Broken Sites	1 New Site	1 New Site
MYO7A	rs7121485	1 Acceptor (+)	+0.34	-400	/	/	/	/	+17 and 1 Broken/4 New Sites	2 Broken Sites	1 New Site

Table 2 - Scores from algorithms applied to deep intronic variants splicing analysis. Matrices for SR proteins (SRp40, SC35, SF2/ ASF, SF2/ASF IgM/BRCA1 and SRp55) from the ESE Finder tool; sequence motifs shown to be differentially present in exons and introns, such as the RESCUE-ESE hexamers, the putative 8-mer ESE and ESS identified by Zhang and Chasin, the ESR sequences identified by Goren and co-workers, and the exon-identity elements (EIE) and intron-identity elements (IIE) defined by Zhang and co-workers. For the silencer sequences identified by Sironi and colleagues and the ESS decamers, a proprietary algorithm was applied to use the crude data.

4. Discussion

Retinitis pigmentosa is a widely heterogeneous group of diseases, with extremely varied symptoms and genetics. Currently, less than 50% of RP types is attributable to known genes, whereas the rest of the molecular impairments causing this condition are still unidentified, especially in populations where few genetic screenings have been performed [14]. The innovative Next Generation Sequence permitted us to investigate the whole genome of proband, allowing the identification of new potential associated gene variants. After several filtering processes, most of the false positive and negative results were discarded, leaving us with 15 variants from 6 genes (EYS, PPEF2, RNF144B, RDH13, FLT3 and MYO7A) as serious causative candidates. An "eye-related" pathway analysis was then carried out in order to determine the real involvement of all the remaining variants in the etiopathogenesis of the unknown-origin Retinitis pigmentosa. EYS was found in the ciliary axoneme, which suggested that it could play an important role in the organization/function of microtubule structures, such as the primary cilium [15]. Furthermore, EYS is also considered vital for the correct activity of cones [15]. Interestingly, the inner segment ellipsoid band length (ISe) of several RP patients with EYS mutations resulted shortened during a 5 year of observation [16]. Moreover, variants in EYS were associated to several

retinal dystrophies in several populations, but never in an Italian one. Despite this, only coding sequence variations were linked to retinal diseases, although it is known that EYS has four isoforms expressed in the retina, regulated by alternative splicing [15]. Protein phosphatase with EF-hand domain 2 (PPEF2) is a potent negative regulator of apoptosis signal-regulating kinase 1 (ASK1), a MAP kinase kinase kinase implicated, among others, in neurodegenerative diseases, like CCM2 [17], and MAPK1[18], involved in the stress- and Mitogen-activated protein kinase signaling cascade. ASK1 is activated by oxidative stress and induces pro-apoptotic or inflammatory signaling. PPEF2 expression may thus correlate with modifications in intracellular metabolism (especially of phosphorus, like in diabetes [19]), stress protective responses (like several co-receptors such as Klotho [20], acting as CCR5 during HIV infection [21]), cell survival, growth, proliferation, or neoplastic transformation [22]. RNF144B, an IBR-type RING-finger E3 ubiquitin ligase, regulates the levels of the pro-apoptotic Bax and protects cells from unprompted Bax activation and cell death. Downregulation of RNF144B induces increased cellular levels and accumulation of the active form of Bax [23]. Moreover, in the regulation of p53-dependent apoptosis, the miR-100 antagonism inhibits ubiquitin-mediated p53 protein degradation by activating RNF144B [24]. Retinol dehydrogenase 13 (RDH13) is a recently discovered short-chain dehydrogenase/reductase, related to microsomal retinoid oxidoreductase RDH11. Retinol dehydrogenases (RDHs) reduce all-trans retinal to all-trans retinol after bleaching of visual pigment in vertebrate photoreceptors. The localization of RDH13 on the outer side of the inner mitochondrial membrane suggests that it may protect mitochondria against oxidative stress associated with the highly reactive retinaldehyde produced from dietary β-carotene [25]. The possible inhibition of the mitochondrial apoptosis pathway could protect the retina against acute light-induced retinopathy [26]. Activation of FLT3 with its ligand could inhibit the proliferation of neural progenitor cells and promote neuron survival, along with NGF [27]. Fiz1 (Flt3-interacting zinc-finger protein) acts as transcriptional repressor of neural retina leucine zipper (NRL) function in photoreceptors, playing a possible role in retina impairment [27]. Myosin VIIA (MYO7A), whose mutations are known to be causative of Usher's Syndrome, is localized in retinal pigmented epithelial (RPE) cells, where it plays a fundamental role in organelle motility and in light-dependent translocation of the visual cycle enzyme RPE65 [28]. A small quantity of myosin VIIA is also associated with the connecting cilium of photoreceptor cells, probably contributing to maintaining a proper diffusion barrier [29]. Interestingly, splicing variants of MYO7A have been analyzed in the past, and several could determine mild forms of retinopathy [30]. The present study highlights the possible negative role of intron variants in splicing events. The sequences that allow the recognition of splice sites are called exonic or intronic splicing enhancers (ESE or ISE), recognized by proteins belonging to the SR family. In addition, the sequences that mask those sites are called exonic or intronic splicing silencers (ESS or ISS), and are recognized by heterogeneous nuclear ribonucleoproteins (hnRNPs). Therefore, the selection of a given splice site (and, consequently, the possibility of alternative splicing), depends on the presence of ESE, ISE, ESS or ISS sequences, and on the availability of the proteins that bind them. In view of these considerations, it is clear that alterations in the nucleotide sequence of a gene can cause the abolition of enhancer sequences or, on the other hand, the creation of silencer sequences, responsible for the lack of recognition of canonical splice sites. Moreover, mutations in the nucleotide sequence could lead to a removal of the canonical sites and the creation of new cryptic splice sites. Variants in EYS (rs149849078 and rs71638759) were postulated to brake exonic ESE sites, as well as PPEF2 rs1976518 and RDH13 rs2569513, while exonic ESS sites could be destroyed by FLT3 rs17086226 or created by the RDH13 polymorphism and RNF144B rs1886248. The latter, furthermore, could be involved in the activation of an exonic cryptic donor site. Less deleterious intronic ESE sites could be created by PPEF2 rs12498639 and the previously cited FLT3 variant, while the PPEF2 rs1566975 is also involved in breaking an intron ESS site, together with MYO7A rs2276283. The other deep intronic variants, characterized by a more intricate splicing alteration pattern, should also determine significant modifications in this process. The balance impairment caused by the simultaneous presence of all analyzed variants could determine an influx of altered proteins, which might impair the trafficking through the photoreceptor-connecting cilium (EYS and MYO7A) and increase oxidative stress (RDH13) that, along with the pro-apoptotic action determined by PPEF2, RNF144B and FLT3 alterations, could lead to photoreceptor death and the onset of retinitis pigmentosa. Subsequent studies already underway will generate functional assays to confirm the in silico results also in in vitro and in vivo studies.

5. Conclusion

Overall, the analyzed nucleotide sequence alterations constitute a very specific group of variants, which can highlight the importance of variations not considered crucial before. The involvement of little- or never-considered genes and a new role of splicing alteration events may offer new insights into the diagnostics of unknown forms of retinitis pigmentosa, in addition to the new information already partially discovered thanks to the advent of the next-generation sequencing technique.

References

1. Sorrentino FS, Gallenga CE, Bonifazzi C, Perri P: A challenge to the striking genotypic heterogeneity of retinitis pigmentosa: a better understanding of the pathophysiology using the newest genetic strategies. Eye (Lond) 2016; 30:1542-1548.

2. Chan P, Stolz J, Kohl S, Chiang WC, Lin JH: Endoplasmic reticulum stress in human photoreceptor diseases. Brain Res 2016; 1648:538-541.

3. Khavinson V, Proniaeva VE, Lin'kova NS, Trofimova SV, Umnpv RS: Molecular-physiological aspects of peptide regulation of function of the retina in retinitis pigmentosa. Fiziol Cheloveka 2014; 40:129-34.

4. Nash B M, Wright DC, Grigg JR, Bennetts B, Jamieson RV: Retinal dystrophies, genomic applications in diagnosis and prospects for therapy. Transl Pediatr 2015; 4:139-63.

5. Newman A M, Gallo NB, Hancox LS, Miller NJ, Radeke CM, Maloney MA, Cooper JB, Hageman GS, Anderson DH, Johnson LV, Radeke MJ: Systems-level analysis of age-related macular degeneration reveals global

biomarkers and phenotype-specific functional networks. Genome Med 2012; 4:16.
6. Crisafulli C, Chiesa A, Han C, Lee SJ, Balzarro B, Andrisano C, Sidoti A, Patkar AA, Pae CU, Serretti A: Case-control association study of 36 single-nucleotide polymorphisms within 10 candidate genes for major depression and bipolar disorder. Psychiatry Res 2013; 209:121-3.
7. Fahim AT, Daiger SP, Weleber RG: Retinitis Pigmentosa Overview. In: GeneReviews(R), Edited by RA Pagon, Adam MP, Ardinger HH, et al. Seattle (WA), 1993.
8. Riaz M and Baird PN: Genetics in Retinal Diseases. Dev Ophthalmol 2016; 55:57-62.
9. D'Angelo R, Alafaci C, Scimone C, Ruggeri A, Salpietro FM, Bramanti P, Tomasello F, Sidoti A: Sporadic cerebral cavernous malformations: report of further mutations of CCM genes in 40 Italian patients. Biomed Res Int 2013; 2013:459253.
10. Singh KK, Kumar R, Prakash J, Krishna A: Bardet-Biedl syndrome presenting with steroid sensitive nephrotic syndrome. Indian J Nephrol 2015; 25:300-2.
11. Esposito T, Varriale B, D'Angelo R, Amato A, A. Sidoti A: Regulation of flavin-containing mono-oxygenase (Fmo3) gene expression by steroids in mice and humans. Horm Mol Biol Clin Investig 2014; 20:99-109.
12. Zhao L, Wang F, Wang H, Li Y, Alexander S, Wang K, Willoughby CE, Zaneveld JE, Jiang L, Soens ZT, Earle P, Simpson D, Silvestri G, Chen R: Next-generation sequencing-based molecular diagnosis of 82 retinitis pigmentosa probands from Northern Ireland. Hum Genet 2015; 134:217-30.
13. Bindea G, Mlecnik B, Hackl H, Charoentong P, Tosolini M, Kirilovsky A, Fridman WH, Pages F, Trajanoski Z, Galon J: ClueGO: a Cytoscape plug-in to decipher functionally grouped gene ontology and pathway annotation networks. Bioinformatics 2009; 25:1091-3.
14. Wang X, Feng Y, Li J, Zhang W, Wang J, Lewis RA, L.J. Wong LJ: Retinal Diseases Caused by Mutations in Genes Not Specifically Associated with the Clinical Diagnosis. PLoS One 2016; 11:e0165405.
15. Alfano G, Kruczek PM, Shah AZ, Kramarz B, Jeffery G, Zelhof AC, Bhattacharya SS: EYS Is a Protein Associated with the Ciliary Axoneme in Rods and Cones. PLoS One 2016; 11:e0166397.
16. Miyata M, Ogino K, Gotoh N, Morooka S, Hasegawa T, Hata M, N. Yoshimura N: Inner segment ellipsoid band length is a prognostic factor in retinitis pigmentosa associated with EYS mutations: 5-year observation of retinal structure. Eye (Lond) 2016; 30:1588-1592.
17. D'Angelo R, Scimone C, Rinaldi C, Trimarchi G., Italiano D, Bramanti P, Amato A, Sidoti A: CCM2 gene polymorphisms in Italian sporadic patients with cerebral cavernous malformation: a case-control study. Int J Mol Med 2012; 29:1113-20.
18. Calati R, Crisafulli C, Balestri M, Serretti A, Spina E, Calabro M, Sidoti A, Albani D, Massat I, Hofer P, Amital D, Juven-Wetzler A, Kasper S, Zohar J, Souery D, Montgomery S, J. Mendlewicz J: Evaluation of the role of MAPK1 and CREB1 polymorphisms on treatment resistance, response and remission in mood disorder patients. Prog Neuropsychopharmacol Biol Psychiatry 2013; 44:271-8.
19. Romano L, Scuteri A, Gugliotta T, Romano P, De Luca G, Sidoti A, Amato A: Sulphate influx in the erythrocytes of normotensive, diabetic and hypertensive patients. Cell Biol Int 2002; 26:421-6.
20. Farinelli P, Arango-Gonzalez B, Volkl J, Alesutan I, Lang F, Zrenner E, Paquet-Durand F, Ekstrom PA: Retinitis Pigmentosa: over-expression of anti-ageing protein Klotho in degenerating photoreceptors. J Neurochem 2013; 127:868-79.
21. Sidoti A, D'Angelo R, Rinaldi C, De Luca G, Pino F, Salpietro C, Giunta DE, Saltalamacchia F, Amato A: Distribution of the mutated delta 32 allele of the CCR5 gene in a Sicilian population. Int J Immunogenet 2005; 32:193-8.
22. Kutuzov MA, Bennett N, Andreeva AV: Protein phosphatase with EF-hand domains 2 (PPEF2) is a potent negative regulator of apoptosis signal regulating kinase-1 (ASK1). Int J Biochem Cell Biol 2010; 42:1816-22.
23. Benard G, Neutzner A, Peng G, Wang C, Livak F, Youle RJ, Karbowski M: IBRDC2, an IBR-type E3 ubiquitin ligase, is a regulatory factor for Bax and apoptosis activation. EMBO J 2010; 29:1458-71.
24. Yang G, Gong Y, Wang Q, Wang L, Zhang X: miR-100 antagonism triggers apoptosis by inhibiting ubiquitination-mediated p53 degradation. Oncogene 2016.
25. Belyaeva OV, Korkina OV, Stetsenko AV, Kedishvili NY: Human retinol dehydrogenase 13 (RDH13) is a mitochondrial short-chain dehydrogenase/reductase with a retinaldehyde reductase activity. FEBS J 2008; 275:138-47.
26. Wang H, Cui X, Gu Q, Chen Y, Zhou J, Kuang Y, Wang Z, Xu X: Retinol dehydrogenase 13 protects the mouse retina from acute light damage. Mol Vis 2012; 18:1021-30.
27. Mitton KP, Swain PK, Khanna H, Dowd M, Apel IJ, Swaroop A: Interaction of retinal bZIP transcription factor NRL with Flt3-interacting zinc-finger protein Fiz1: possible role of Fiz1 as a transcriptional repressor. Hum Mol Genet 2003; 12:365-73.
28. Goldenberg-Cohen N, Banin E, Zalzstein Y, Cohen B, Rotenstreich Y, Rizel L, Basel-Vanagaite L, Ben-Yosef T: Genetic heterogeneity and consanguinity lead to a "double hit": homozygous mutations of MYO7A and PDE6B in a patient with retinitis pigmentosa. Mol Vis 2013; 19:1565-71.
29. Williams DS, Lopes VS: The many different cellular functions of MYO7A in the retina. Biochem Soc Trans, 2011; 39:1207-10.
30. Ben Rebeh I, Moriniere M, Ayadi L, Benzina Z, Charfedine I, Feki J, Ayadi H, Ghorbel A, Baklouti F, Masmoudi S: Reinforcement of a minor alternative splicing event in MYO7A due to a missense mutation results in a mild form of retinopathy and deafness. Mol Vis 2010; 16:1898-906.

.